DOI:
10.1016/j.jid.2017.05.041

Document Version
Peer reviewed version

Accepted Manuscript

Caveolin-1 controls hyperresponsiveness to mechanical stimuli and fibrogenesis-associated RUNX2 activation in keloid fibroblasts

Chao-Kai Hsu, Hsi-Hui Lin, Hans I-Chen Harn, Rei Ogawa, Yang-Kao Wang, Yen-Ting Ho, Wan-Rung Chen, Yi-Chao Lee, Julia Yu-Yun Lee, Shyh-Jou Shieh, Chao-Min Cheng, John A. McGrath, Ming-Jer Tang

PII: S0022-202X(17)32933-0

DOI: 10.1016/j.jid.2017.05.041

Reference: JID 1060

To appear in: *The Journal of Investigative Dermatology*

Received Date: 13 September 2016

Revised Date: 20 May 2017

Accepted Date: 30 May 2017

Please cite this article as: Hsu C-K, Lin H-H, I-Chen Harn H, Ogawa R, Wang Y-K, Ho Y-T, Chen W-R, Lee Y-C, Yu-Yun Lee J, Shieh S-J, Cheng C-M, McGrath JA, Tang M-J, Caveolin-1 controls hyperresponsiveness to mechanical stimuli and fibrogenesis-associated RUNX2 activation in keloid fibroblasts, *The Journal of Investigative Dermatology* (2017), doi: 10.1016/j.jid.2017.05.041.

Caveolin-1 controls hyperresponsiveness to mechanical stimuli and fibrogenesis-associated RUNX2 activation in keloid fibroblasts

Chao-Kai Hsu[1,2,3*], Hsi-Hui Lin[4*], Hans I-Chen Harn[3,4], Rei Ogawa[5], Yang-Kao Wang[6], Yen-Ting Ho[4], Wan-Rung Chen[2], Yi-Chao Lee[7], Julia Yu-Yun Lee[1,3], Shyh-Jou Shieh[8], Chao-Min Cheng[9], John A. McGrath[10] and Ming-Jer Tang[3,4]

[1]Institute of Clinical Medicine, College of Medicine, National Cheng Kung University, Tainan, Taiwan

[2]Department of Dermatology, National Cheng Kung University Hospital, College of Medicine, National Cheng Kung University, Tainan, Taiwan

[3]International Research Center of Wound Repair and Regeneration, National Cheng Kung University, Tainan, Taiwan

[4]Department of Physiology, College of Medicine, National Cheng Kung University, Tainan, Taiwan

[5]Department of Plastic, Reconstructive and Aesthetic Surgery, Nippon Medical School, Tokyo, Japan

[6]Department of Anatomy, National Cheng Kung University Hospital, College of Medicine, National Cheng- Kung University, Tainan, Taiwan

[7]Ph.D. Program for Neural Regenerative Medicine, College of Medical Science and Technology, Taipei Medical University, Taipei, Taiwan

[8]Department of Surgery, College of Medicine, National Cheng Kung University, Tainan, Taiwan

[9]Institute of Nanoengineering and Microsystems, National Tsing Hua University, Hsinchu, Taiwan

[10]St John's Institute of Dermatology, King's College London (Guy's Campus), London, UK

* These authors contributed equally to this work

Correspondence:

Ming-Jer Tang, M.D., Ph.D.

E-mail: mjtang1@mail.ncku.edu.tw

Address: Department of Physiology, College of Medicine, National Cheng-Kung University, 1 Da-Hsueh Road, Tainan 70101, Taiwan.

Telephone: 886-6-235-3535, ext. 5425

Fax: 886-6-236-2780

Short title: Mechanobiology of Keloid Fibroblasts

Word counts: main text, 3460 words

Figure counts: 6

Table counts: 0

Key words: keloid/caveolin-1/RUNX2/mechanobiology/fibrosis

Abbreviations: AFM, atomic force microscopy; CAV1, caveolin-1; COL, collagen; ECL, enhanced chemiluminescence; ECM, extracellular matrix; FN, fibronectin; HDAC, histone deacetylase; IHC, immunohistochemistry; IPA, ingenuity pathway analysis; KFs, keloid fibroblasts; MLC, myosin light chain; NFs, normal fibroblasts; PA, polyacrylamide; PDMS, polydimethylsiloxane; siNC, non-targeting control siRNA; siRNA, short interfering RNA; TCP, tissue culture plastic; TSA, trichostatin A

ABSTRACT

Keloids are pathological scars characterized by excessive extracellular matrix production that are prone to form in body sites with increased skin tension. Caveolin-1 (CAV1), the principal coat protein of caveolae, has been associated with the regulation of cell mechanics, including cell softening and loss of stiffness sensing ability in NIH3T3 fibroblasts. Although CAV1 is present in low amounts in keloid fibroblasts (KFs), the causal association between CAV1 downregulation and its aberrant responses to mechanical stimuli remain unclear. In this study, atomic force microscopy showed that KFs were softer than normal fibroblasts with a loss of stiffness sensing. The decrease of CAV1 contributed to the hyperactivation of fibrogenesis-associated RUNX2, a transcription factor germane to osteogenesis/chondrogenesis, and increased migratory ability in KFs. Treatment of KFs with trichostatin A (TSA), which increased the acetylation level of histone H3, increased CAV1 and decreased RUNX2 and fibronectin. TSA treatment also resulted in cell stiffening and decreased migratory ability in KFs. Collectively, these results suggest a novel role for CAV1 downregulation in linking the aberrant responsiveness to mechanical stimulation and extracellular matrix accumulation with the progression of keloids, findings that may lead to new developments in the prevention and treatment of keloid scarring.

INTRODUCTION

Keloids occur as a result of abnormal wound healing, and are characterized by excessive deposition of collagen in the dermis with extension of scar tissue beyond the original borders of wounds (Bran *et al.*, 2009; Niessen *et al.*, 1999). Pathologically, keloids are characterized by thick hyalinized eosinophilic collagen fibers (keloidal collagen) and a horizontal, tongue-like advancing edge in the upper dermis (Jumper *et al.*, 2015; Lee *et al.*, 2004). The etiology and molecular mechanism of keloid formation have not been fully elucidated, and effective prevention or treatment for keloids is still lacking (Tziotzios *et al.*, 2012).

Human skin is a highly specialized mechanoresponsive organ, which continually senses and adapts to various mechanical stimuli (Ogawa and Hsu, 2013; Wong *et al.*, 2011). Keloids tend to form in areas of the body subjected to increased skin tension or stiffness, such as the presternum and shoulders (Ogawa *et al.*, 2011). A simulated finite element analysis showed that mechanical stimulation (i.e. skin-stretching tension) strongly influences the cellular behavior that leads to keloid growth (Akaishi *et al.*, 2008). Thus, decreasing skin tension has been suggested as potentially beneficial for treating keloids (Ogawa *et al.*, 2011).

As observed for chemical stimuli, matrix stiffness also has a large impact on the

regulation of cell behavior, such as survival, proliferation, differentiation, and migration (Stroka and Konstantopoulos, 2014; Wang *et al.*, 2007). Moreover, several proteins, such as FAK and integrins, are found to play key roles in the mechanosensing and mechanotransduction of cells (Jansen *et al.*, 2015). Recently, we found that decreased Caveolin-1 (CAV1) contributes to cell softening and loss of rigidity sensing ability in Ha-Ras^{V12}-transformed fibroblasts (Lin *et al.*, 2015). CAV1, a major component of caveolae, plays an important role in signal transduction, membrane traffic and cholesterol transport (Boscher and Nabi, 2012). In addition to its primary role as a tumor suppressor, CAV1 has been linked to the regulation of focal adhesions and integrin-mediated actin remodeling, which have been widely studied for their role in mechanotransduction (Nethe and Hordijk, 2011; Radel *et al.*, 2007; Yang *et al.*, 2011a). In various fibrotic disorders, including idiopathic pulmonary fibrosis, systemic sclerosis, and keloids, Cav1 was downregulated (Del Galdo *et al.*, 2008; Wang *et al.*, 2006; Zhang *et al.*, 2011). Collectively, we speculate that, in keloid fibroblasts (KFs), a decrease in CAV1 may result in an aberrant response to the mechanical stimuli from the local environment.

Epigenetic mechanisms are important in regulating the wound healing processes, including keratinocyte proliferation, differentiation, and migration, together with dermal regeneration and neoangiogenesis (Lewis *et al.*, 2014). The

histone deacetylase (HDAC) inhibitor, trichostatin A (TSA), has potent antifibrogenic effects in a mouse model of bleomycin-induced skin fibrosis (Huber *et al.*, 2007). Treatment of fibroblasts with TSA causes abrogated TGF-β1-induced collagen gene expression (Ghosh *et al.*, 2007; Rombouts *et al.*, 2002). Russell *et al.* (2010) found epigenetic modifications in KFs that include an altered pattern of DNA methylation and histone acetylation. Although HDAC inhibition by TSA has been shown to inhibit collagen synthesis of KFs (Diao *et al.*, 2011), the molecular mechanism underpinning this response remains unknown.

Our study aims to understand the mechanical properties of KFs and the mechanisms underlying the hyperresponsiveness of KFs to mechanical stimuli.

RESULTS

Keloid tissues are stiffer than normal dermal tissues, whereas keloid fibroblasts (KFs) are softer than normal dermal fibroblasts

Comparison of ECM levels in dermal tissues from keloid lesions and normal dermis revealed a relative increase in fibronectin (FN), and collagen (COL)1A1, COL3A1, and COL11A1 in the keloid tissues (Figure 1a and b). Atomic force microscopy (AFM) indentation measurements showed that keloid tissues (14213 ± 1047 Pa) were approximately 10-fold stiffer than normal skin tissue (2406 ± 1035

Pa) ($p<0.01$) (Figure 1c and Supplementary Figure S1). This ECM accumulation in keloid lesions could be due to a corresponding increase in the amounts of ECM produced by the KFs (Figure 1d and e). However, at the cellular level, KFs (1133 ± 77 Pa) were softer than normal fibroblasts (NFs) (1539 ± 113 Pa) from healthy subjects ($p<0.01$) (Figure 1f and g).

RUNX2 is a potential key regulator for ECM overproduction in keloids

We analyzed the microarray results from 7 Japanese patients with keloids. A total of 345 upregulated genes (>4-fold), 86 downregulated genes (<-4-fold) and 15 transcription regulators were identified in the keloid tissue compared with adjacent normal tissue (discarded skin as “dog ear” for aesthetic reason). Using Ingenuity Pathway Analysis (IPA) software (http://www.ingenuity.com), canonical pathway analysis revealed that the pathway of “the role of osteoblasts, osteoclasts, and chondrocytes in rheumatoid arthritis” was the most important signaling pathway, highlighting 17 significantly upregulated and one downregulated gene from the comparative dataset (Supplementary Figure S2). The upstream regulatory analysis revealed three key transcription regulators in the keloid group, including runt-related transcription factor 2 (RUNX2), NK3 homeobox 2 (NKX3-2), and MLX-interacting protein-like (MLXIPL) (Supplementary Table S1). Among these, RUNX2 plays a

vital role in regulating the downstream ECM proteins, including COL11A1, which is predominantly found in cartilage (Figure 2a). The expression of RUNX2 in dermal tissues was examined by immunohistochemistry on various tissue sections of normal skin, normal scar, hypertrophic scar and keloid tissue (Figure 2b). Among these tissues, the highest percentage of fibroblasts with nuclear RUNX2, was found in keloid tissue (Figure 2c). Immunoblotting of lysates from normal and keloid tissues showed that pRUNX2 (the active form of RUNX2) and RUNX2 were upregulated, albeit showing no statistical significance, in keloid tissue (Figure 2d and e). However, NFs expressed similar levels of pRUNX2 and RUNX2 as compared to KFs after culture on tissue culture plastic (TCP) dish (Figure 2f and g). The role of RUNX2 in the overproduction of ECMs in KFs was validated using short interfering RNA (siRNA) to silence RUNX2. Suppression of RUNX2 downregulated the mRNA level of FN and COL11A1 in KFs (Supplementary Figure S3). Altogether, these data suggest that the highly active RUNX2 in KFs could be involved in excessive ECM production in keloid tissue.

Hyperresponsiveness of KFs to dermal tissue-equivalent matrix stiffness causes increased expression of RUNX2 and COL11A1

It is known that primary cells cultured on TCP dish with a physical stiffness

$>10^9$ (G) Pa, are spontaneously activated towards myofibroblast differentiation (Achterberg *et al.*, 2014; Chen *et al.*, 2014). We postulate that the increased RUNX2 expression in NFs is associated with the extreme change in matrix stiffness, from soft dermal tissue to stiff TCP dish, during primary culture. The effects of matrix stiffness on the expression of RUNX2 were investigated by culturing the primary dermal fibroblasts on stiff TCP dish (>G Pa), 2 kPa polyacrylamide (PA) gel (normal dermis-equivalent stiffness) and 20 kPa PA gel (keloid-equivalent stiffness). As shown in Figure 3a and b, the expression of nuclear RUNX2 was increased with increasing matrix stiffness in both NFs and KFs. However, KFs expressed higher nuclear RUNX2 than NFs did on whichever condition. The expression of FN in KFs was prominently elevated with increasing matrix stiffness (Figure 3c). Nevertheless, the expression of FN in NFs was only slightly enhanced, despite culturing on the TCP dish. We further performed explant culture of fibroblasts on type I collagen-coated PA gels of 2 and 20 kPa to diminish the stiff matrix-induced RUNX2 activation during primary culture. The mRNA level of RUNX2 and several ECM genes were evaluated on Day 3. As shown in Figure 3d and 3e, NFs derived from explant culture on 2 and 20 kPa PA gels were devoid of RUNX2 and COL11A1. The mRNA levels of FN and COL3A1 of NFs were low on the 2 kPa PA gel and increased slightly on the 20 kPa PA gel. KFs derived from explants cultured

on 2 kPa PA gels expressed a higher RUNX2, COL11A1, FN, and COL3A1 mRNA level than NFs did, which were intensified on 20 kPa PA gels. Collectively, these data show that physiologically-equivalent mechanical culture conditions suppress the expression of fibrosis-associated RUNX2 and COL11A1 of NFs in comparison with conventional stiff TCP. Moreover, it seems that KFs show hyperresponsiveness to dermal tissue-equivalent matrix stiffness, which causes increased expression of RUNX2 and COL11A1.

Decreased CAV1 is associated with cell softening and the upregulation of fibrogenesis-associated RUNX2 and migratory ability in KFs

Although keloids are categorized as a benign fibroproliferative lesions selectively occurring in the dermis, their aggressive and recurrent behavior resembles that of malignant tumors. Our previous study demonstrated that decreased CAV1 contributes to changes in the cell mechanics of cancer cells (Lin *et al.*, 2015). The cDNA microarray data revealed that *CAV1* level was downregulated in keloid tissues (-1.548) compared with adjacent normal tissue. Thus, it is important to understand whether CAV1 is also involved in the pathogenesis of keloids, particularly from a mechanobiological perspective. Immunofluorescence showed that CAV1 was expressed in the cytoplasm and cell membrane of dermal fibroblasts

of normal skin, normal scar, and a perilesional normal skin of keloid tissue (Supplementary Figure S4). In contrast, CAV1 expression was markedly decreased in keloid lesions (Supplementary Figure S4) and KFs (Figure 4a). The potential association of CAV1 with cell mechanics of human dermal fibroblasts was studied using siRNA to knockdown *CAV1* in NFs (Figure 4a and b). *CAV1* knockdown caused softening of NFs (Figure 4c). When cultured on matrices of varying stiffness, siNC (non-targeting control siRNA)-treated NFs altered their stiffness, but siCAV1-treated NFs and KFs did not (Figure 4d). The results indicated the loss of stiffness sensing ability in siCAV1-treated NFs and KFs. Furthermore, *CAV1* knockdown increased the expression and nuclear translocation of RUNX2 (Figure 4a, b, e, and f), and increased FN expression (Figure 4a and b) in NFs. Knockdown of CAV1 did not change the expression pattern of nuclear RUNX2 in NFs or KFs grown on matrices of 20 kPa and 2 kPa (Figure 4g). However, si*CAV1*-treated NFs showed higher percentage of cells with nuclear RUNX2 when cultured on 2 kPa PA gel, as compared with siNC-treated NFs. These data suggest that a decrease in CAV1 might contribute to keloid pathogenesis via elevating fibrogenic RUNX2 expression. Immunostaining results showed that dermal fibroblasts in normal and peripheral normal skin near the keloid lesion, expressed high CAV1 and extremely low RUNX2, while dermal fibroblasts in keloid lesions express low CAV1 and high

RUNX2 (Figure 4h). Pearson's correlation analysis revealed that CAV1 was negatively correlated with RUNX2 in keloid lesions (Figure 4i).

One characteristic of keloids is their ability to continually migrate beyond the original border of a wound (Witt *et al.*, 2008). *In vitro* studies revealed that KFs migrated faster and displayed a higher total force and force per post than NFs (Harn *et al.*, 2015; Witt *et al.*, 2008). Also, Cav1-depleted NIH3T3 fibroblasts displayed increased cell migration (Lin *et al.*, 2015). Here, we found that *CAV1* knockdown by siRNA increased migratory ability (Figure 5a and Supplementary Figure S5) and force per post of NFs (siCav/NFs vs. siNC/NFs: 4.18 ± 0.14 nN vs. 3.53 ± 0.08 nN) (Figure 5b and c). Further, both MLC2 protein and MLC2 phosphorylation, the relevant mediators of transcellular contractility (Iwabu *et al.*, 2004), were markedly increased in KFs and in CAV1-depleted NFs (Figure 5d and e). Collectively, these data show that KFs are softer and migrate faster than NFs, which may correlate with the decrease in CAV1.

TSA, an HDAC inhibitor, inhibited histone deacetylase, increased CAV1 and decreased RUNX2 in KFs

Considering that CAV1 downregulation only occurs in actual keloid lesions, CAV1 might be under epigenetic regulation. HDAC2, an epigenetically-regulated

enzyme, is strikingly upregulated in keloid scars (Fitzgerald O'Connor *et al.*, 2012). Moreover, inhibition of HDAC by TSA diminished collagen synthesis in KFs (Diao *et al.*, 2011). Here, treatment of KFs with TSA increased acetylation of K9 of histone H3 (histone H3AK9) and CAV1 expression (Figure 6a-d). Consequently, TSA-treated KFs showed the phenotype toward normal, including decreased expression of RUNX2 and FN (Figure 6e and f), migratory ability (Figure 6g), and increased cell stiffness (Figure 6h). Finally, TSA-treated KFs showed decreased percentage of cells with nuclear RUNX2 when cultured on 2 kPa PA gel (Figure 6i). Collectively, these data suggest the important role of epigenetics-modulated CAV1 in the pathogenesis of keloid scars.

DISCUSSION

In this study, we showed that CAV1 downregulation played a critical role in the pathogenesis of keloids. The finding is consistent with those from Zhang et al. (2011) who showed that CAV1, antagonizing profibrotic processes by decreasing TGF-β receptor type I and Smad2/3 phosphorylation, was markedly decreased in keloid-derived fibroblasts. Given CAV1 levels in keloid lesions were substantially lower in comparison with perilesional skin of the keloid (Supplementary Figure S4) and HDACs inhibitor TSA increased CAV1 in KFs (Figure 6a), epigenetic modifications involvement in the decrease of CAV1 are suggested. *In vivo* studies of

mouse and human skin wounds revealed that HDAC2 is markedly increased in both normal and keloid scar tissues (Fitzgerald O'Connor *et al.*, 2012). Whether the heightened HDAC2 is relevant to epigenetically downregulated CAV1 in keloid lesions remains unknown. Given the normal scar tissues normally expressed CAV1 (Supplementary Figure S4), it is possible that other epigenetic modifying enzymes dominate the CAV1 downregulation or other factors are required to potentiate the action of HDAC2 in keloid lesions.

CAV1 has been implicated in pathological conditions of abnormal collagen expression in the skin. When Cav1 was knockout, mice exhibited scleroderma-like pathological skin features, characterized by upregulated expression of dermal collagens (Castello-Cros *et al.*, 2011), or had greater bone size and stiffness, along with an increase in alkaline phosphatase protein and expression of osterix and Runx2 (Rubin *et al.*, 2007). In human dermal fibroblasts, CAV1 inhibition by methyl-β-cyclodextrin led to upregulation of collagen expression (Lee *et al.*, 2015). In this study, the Ingenuity Pathway Analysis (IPA) data show that “the role of osteoblasts, osteoclast, and chondrocytes in rheumatoid arthritis” is the most important signaling pathway in keloids (Supplementary Figure S2), which are consistent with those from Naitoh et al. (2005) who showed that gene expression in human keloids is altered from dermal to chondrocytic and osteogenic lineage.

Noteworthy, RUNX2, the osteogenesis-specific transcription factor, is ectopically expressed in KFs *in vitro* and *in vivo* (Figure 4) (Naitoh, 2005). In osteoblasts, Runx2 was found to be a target of mechanical signals mediated by Ras/ERK1/2 MAPK signaling (Kanno *et al.*, 2007; Ziros *et al.*, 2002). Runx2 was also shown to be an inducer of aortic fibrosis and stiffness (Raaz *et al.*, 2015). Silencing *CAV1* with siRNA in NFs, increased RUNX2 expression (Figure 4a), whereas enhancing CAV1 with TSA treatment in KFs suppressed RUNX2 expression (Figure 6a and b), suggesting that the repressive role of CAV1 in RUNX2 expression. Cav1, the main component of caveolae, have been shown to serve as scaffolds for a variety of signaling molecules and negatively regulate signal penetrance (Boscher and Nabi, 2012). Accordingly, silencing *CAV1* might relief the signals that lead to the expression RUNX2 in keloids. However, the expression of RUNX2 was also reported to be modulated by HDAC inhibitors in different cell types. Saito et al. (2013) showed cyclic tensile strain-induced expression of RUNX2 was suppressed by TSA in human chondrocytes. Conversely, Cho et al. (2005) showed that valproic acid treatment increased RUNX2 expression and osteogenic differentiation of human bone marrow stromal cells and human adipose tissue-derived stromal cells. This discrepancy may be explained by cell type differences, which initiate various signaling pathway. Although we suggest that TSA upregulated-CAV1 play a critical role in the

suppression of RUNX2, we cannot rule out the possibility that TSA treatment suppresses RUNX2 expression bypassing CAV1 restoration.

Expression of COL11A1 is very low or absent in normal skin. In several types of cancer, high expression of COL11A1 occurred in the invasive carcinoma and activated stromal cells of the desmoplastic reaction, and this expression is correlated with carcinoma aggressiveness and progression, and lymph node metastasis (Raglow and Thomas, 2015; Vazquez-Villa et al., 2015). Here, the cDNA microarray data indicates that *COL11A1* is the most highly upregulated collagen gene in KFs related to NFs, which coincided with previous findings (Chen et al., 2003, Naitoh et al., 2005, Seifert et al., 2008). RUNX2 knockdown by siRNA significantly decreased *COL11A1* (Supplementary Figure S3), suggesting that RUNX2 is vital for the expression of COL11A1 in keloid fibroblasts. Although the function of COL11A1 in keloid remain unknown, it is plausible that COL11A1 might confer keloid fibroblasts the invasive ability to spread outside the original injury site. However, more in-depth studies are needed to determine the mechanism through which COL11A1 influences keloid fibroblasts behavior. In summary, RUNX2/COL11A1 expression might be a remarkable biomarker of keloid fibroblasts and an ideal target for future therapies in keloid.

Matrices of physiologic stiffness potently inhibit normal cell proliferation (Klein

et al., 2009; Lin *et al.*, 2015) and TGF-β-induced fibrosis (Chen *et al.*, 2014; Leight *et al.*, 2012), thus, regulation of tissue stiffness level is fundamental for the physiological function of organs. Discordance of cell and matrix stiffness has been hypothesized to contribute to the pathogenesis of cancer and scarring (Janmey and Miller, 2011). Here, we found that KFs shared similar mechanical phenotypes with cancer cells, including cell softening and loss of stiffness sensing ability due to decreased CAV1 (Lin *et al.*, 2015). Cav1 is linked to the formation of actin cap, which dominates cell stiffness and mechanosensing in NIH3T3 fibroblasts (Lin *et al.*, 2015). However, immunostaining results showed that microtubule polymerization, but not actin cap organization, was weakened in KFs compared to NFs (data not shown). Microtubules function as rigid struts and contribute to cytoskeletal stiffness as well as cellular contractions. Kawabe et al. (2006) demonstrated that downregulation of caveolins attenuated microtubule polymerization, which indirectly regulates cellular signaling. Microtubule disruption has been reported to increase the isometric cell force, an effect attributed to either change in intracellular Ca^{2+} (Paul *et al.*, 2000), which regulates actomyosin contractility, or increases in MLC phosphorylation, resulting from the release of tubulin monomers (Birukova *et al.*, 2004; Kolodney and Elson, 1995). Altogether, it seems reasonable to propose that decreased CAV1 may inhibit microtubule polymerization, which decreases cell stiffness (Figure 4c) but

increases contractile forces, resulting from MLC2 activation (Figure 5b-e) in KFs. Cells sense stiffness through mechanosensing of strains on their cytoskeletons by outside-in signaling mechanisms (Discher *et al.*, 2005). These forces, exerted on the cells, trigger further changes in morphology and phenotype (Engler *et al.*, 2006; Goldmann, 2014). Although CAV1 is linked to the stiffness sensing ability of KFs, the underlying mechanism remains unclear. Previous studies showed that β1 integrin-mediated mechanotransduction is mediated by caveolae domains (Radel *et al.*, 2007; Wei *et al.*, 2008). CAV1 has been shown to inhibit metastatic potential in melanomas through suppression of the integrin/Src/FAK signaling pathway (Trimmer *et al.*, 2010). Suarez *et al.* (2013) found that three specific tension-related genes and proteins (Hsp27, α2β1 integrin, and PAI-2), are overexpressed in keloids and regulate ECM production. Altogether, it is plausible that CAV1 interacts with the integrin/FAK network to regulate the mechanotransduction of the skin. There are some animal models developed to mimic hypertrophic scar (Ibrahim *et al.*, 2014; Wong *et al.*, 2011) or keloid (Lee *et al.*, 2016). It would be interesting to further test our hypothesis through these *in vivo* models.

In conclusion, we highlight a novel role of CAV1 in the progression of keloids (see also Schematic model in Supplementary Figure S5). Epigenetically decreased CAV1 increases fibrogenesis-associated RUNX2 and alters cell mechanics,

including cell softening, loss of stiffness sensing ability, and increase in contractile forces. Consequently, keloid-derived fibroblasts exhibit hyperresponsiveness to both normal dermis-equivalent stiffness (2 kPa) and pathological keloid-equivalent stiffness (20 kPa) or have established an activated state of fibrogenesis-associated RUNX2 that is independent of mechanical cues. These results could explain why KFs produce excessive ECM and prominently migrate into the surrounding normal dermal tissue, thus generating the main clinicopathologic hallmarks of keloids.

MATERIALS AND METHODS

Human samples

The study was approved by the Institutional Review Board at the National Cheng Kung University Hospital (NCKUH-10105017/BR-100-102). Participants gave their written informed consent, and as detailed in the Supplementary Materials and Methods.

Primary culture of fibroblasts

Fibroblasts were isolated from dermal tissues, according to Zhang *et al*. (2009) and as detailed in the Supplementary Materials and Methods.

Measurements of cell/tissue mechanical properties by AFM

For measurements of cell/tissue stiffness, a JPK NanoWizard II AFM with BioCell (JPK Instruments, Berlin, Germany) was equipped and manipulated as previously described (Chiou *et al.*, 2013; Harn *et al.*, 2015; Lin *et al.*, 2015) and as detailed in the Supplementary Materials and Methods.

Preparation and fabrication of Polyacrylamide (PA) gels

PA gels with uniform stiffness were prepared as previously described (Chen *et al.*, 2014; Lin *et al.*, 2015) and as detailed in the Supplementary Material and Methods. The Young's moduli of the PA gels used, were as follows: 2 and 20 kPa PA gels represented the elastic modulus of normal and keloid dermis, respectively. PA gels from each polymerization batch were checked to verify consistent matrix mechanical properties by AFM.

cDNA microarrays analysis and IPA

The microarray study was approved by the ethical committee at Nippon Medical School, Tokyo, Japan (No.22-11-143) and detailed in the Supplementary Materials and Methods.

Western blot analyses

Cell lysates were harvested in modified RIPA buffer. After sonication, lysates were resolved on SDS-PAGE and analyzed by Western blot as detailed in the

Supplementary Material and Methods.

RT-PCR

Total RNA was extracted from cells using TRIzol reagent (Invitrogen-Molecular Probes, Carlsbad, CA) according to the manufacturer's instructions, and as detailed in the Supplementary Materials and Methods.

Immunofluorescence staining and confocal microscopy

Immunofluorescence staining was performed as previously described (Chen *et al.*, 2015), and as detailed in the Supplementary Materials and Methods.

Immunohistochemistry (IHC)

IHC was performed, as previously described (Lee *et al.*, 2010), and as detailed in the Supplementary Materials and Methods.

Cell transfection with siRNA

The expressions of RUNX2 and CAV1 were knocked down using commercially available RUNX2 and CAV1 siRNA kits purchased from Dharmacom (Upstate, Lake Placid, NY). Fibroblasts at a density of 60% confluence were serum-deprived for 24 hours and then transfected with human RUNX2- and caveolin-1-specifc siRNA or non-targeting control-siRNA using the Lipofectamine

2000 reagent (Invitrogen), according to the manufacturer's protocol.

Wound migration assay

In vitro wound assays were performed using IBIDI culture inserts according to the manufacturer's instructions, and as detailed in the Supplementary Materials and Methods.

Fabrication of micropost arrays and quantification of traction force

PDMS micropost arrays were fabricated using standard microfabrication techniques as previously described (Fu *et al.*, 2010; Lin *et al.*, 2015; Yang *et al.*, 2011b) and detailed in the Supplementary Materials and Methods.

Statistical analysis

Most data are shown as the mean ± SEM of independent experiments. Some data were normalized as described in the figure legends and expressed as mean relative value ± SEM. Analyses of the results used ANOVA and Student's t-tests by GraphPad Prism 3.0 (GraphPad Software, San Diego, CA). Each experiment was repeated at least three times to ensure the validity of the data. Values of $p<0.05$ were considered significant.

CONFLICT OF INTEREST: The authors state no conflict of interest.

ACKNOWLEDGMENTS

We thank Yuan-Yu Hsueh for assistance with tissue sampling. This work was supported by grants of the National Science Council/the Ministry of Science and Technology (NSC 99-2314-B-006-008-MY3 and MOST105-2320-B-006-044 to Dr. Chao-Kai Hsu, MOST103-2320-B-006-044-MY3 to Dr. Ming-Jer Tang), and the grants of National Cheng Kung University Hospital (NCKUH-10105017 and NCKUH-10204011 to Dr. Chao-Kai Hsu).

REFERENCES

Achterberg VF, Buscemi L, Diekmann H, Smith-Clerc J, Schwengler H, Meister JJ, et al. The nano-scale mechanical properties of the extracellular matrix regulate dermal fibroblast function. J Invest Dermatol 2014;134:1862-72.

Akaishi S, Akimoto M, Ogawa R, Hyakusoku H. The relationship between keloid growth pattern and stretching tension: visual analysis using the finite element method. Ann Plast Surg 2008;60:445-51.

Birukova AA, Smurova K, Birukov KG, Usatyuk P, Liu F, Kaibuchi K, et al. Microtubule disassembly induces cytoskeletal remodeling and lung vascular barrier dysfunction: role of Rho-dependent mechanisms. J Cell Physiol

2004;201:55-70.

Boscher C, Nabi IR. Caveolin-1: role in cell signaling. Adv Exp Med Biol 2012;729:29-50.

Bran GM, Goessler UR, Hormann K, Riedel F, Sadick H. Keloids: current concepts of pathogenesis (review). Int J Mol Med 2009;24:283-93.

Castello-Cros R, Whitaker-Menezes D, Molchansky A, Purkins G, Soslowsky LJ, Beason DP, et al. Scleroderma-like properties of skin from caveolin-1-deficient mice: implications for new treatment strategies in patients with fibrosis and systemic sclerosis. Cell Cycle 2011;10:2140-50

Chen W, Fu X, Sun X, Sun T, Zhao Z, Sheng Z. Analysis of differentially expressed genes in keloids and normal skin with cDNA microarray. J Surg Res 2003;113:208-16.

Chen WC, Lin HH, Tang MJ. Regulation of proximal tubular cell differentiation and proliferation in primary culture by matrix stiffness and ECM components. Am J Physiol Renal Physiol 2014;307:F695-707

Chen WC, Lin HH, Tang MJ. Matrix-Stiffness-Regulated Inverse Expression of Kruppel-Like Factor 5 and Kruppel-Like Factor 4 in the Pathogenesis of Renal Fibrosis. Am J Pathol 2015;185:2468-81.

Chiou YW, Lin HK, Tang MJ, Lin HH, Yeh ML. The influence of physical and

physiological cues on atomic force microscopy-based cell stiffness assessment. PloS one 2013;8:e77384.

Cho HH, Park HT, Kim YJ, Bae YC, Suh KT, Jung JS Induction of osteogenic differentiation of human mesenchymal stem cells by histone deacetylase inhibitors. J Cell Biochem 2005;96:533-42.

Del Galdo F, Sotgia F, de Almeida CJ, Jasmin JF, Musick M, Lisanti MP, et al. Decreased expression of caveolin 1 in patients with systemic sclerosis: crucial role in the pathogenesis of tissue fibrosis. Arthritis Rheum 2008;58:2854-65.

Diao JS, Xia WS, Yi CG, Wang YM, Li B, Xia W, et al. Trichostatin A inhibits collagen synthesis and induces apoptosis in keloid fibroblasts. Arch Dermatol Res 2011;303:573-80.

Discher DE, Janmey P, Wang YL. Tissue cells feel and respond to the stiffness of their substrate. Science 2005;310:1139-43.

Engler AJ, Sen S, Sweeney HL, Discher DE. Matrix elasticity directs stem cell lineage specification. Cell 2006;126:677-89.

Fitzgerald O'Connor EJ, Badshah, II, Addae LY, Kundasamy P, Thanabalasingam S, Abioye D, et al. Histone deacetylase 2 is upregulated in normal and keloid scars. J Invest Dermatol 2012;132:1293-6.

Fu J, Wang YK, Yang MT, Desai RA, Yu X, Liu Z, et al. Mechanical regulation of cell function with geometrically modulated elastomeric substrates. Nat Methods 2010;7:733-6.

Ghosh AK, Mori Y, Dowling E, Varga J. Trichostatin A blocks TGF-beta-induced collagen gene expression in skin fibroblasts: involvement of Sp1. Biochem Biophys Res Commun 2007;354:420-6.

Goldmann WH. Mechanosensation: a basic cellular process. Prog Mol Biol Transl Sci 2014;126:75-102.

Harn HI, Wang YK, Hsu CK, Ho YT, Huang YW, Chiu WT, et al. Mechanical coupling of cytoskeletal elasticity and force generation is crucial for understanding the migrating nature of keloid fibroblasts. Exp Dermatol 2015;24:579-84.

Huber LC, Distler JH, Moritz F, Hemmatazad H, Hauser T, Michel BA, et al. Trichostatin A prevents the accumulation of extracellular matrix in a mouse model of bleomycin-induced skin fibrosis. Arthritis Rheum 2007;56:2755-64.

Ibrahim MM, Bond J, Bergeron A, Miller KJ, Ehanire T, Quiles C, et al. A novel immune competent murine hypertrophic scar contracture model: a tool to elucidate disease mechanism and develop new therapies. Wound Repair

Regen 2014;22:755-64.

Israeli-Rosenberg S, Chen C, Li R, Deussen DN, Niesman IR, Okada H, et al. Caveolin modulates integrin function and mechanical activation in the cardiomyocyte. FASEB J 2015;29:374-84.

Iwabu A, Smith K, Allen FD, Lauffenburger DA, Wells A. Epidermal growth factor induces fibroblast contractility and motility via a protein kinase C delta-dependent pathway. J Biol Chem 2004;279:14551-60.

Janmey PA, Miller RT. Mechanisms of mechanical signaling in development and disease. J Cell Sci 2011;124:9-18.

Jansen KA, Donato DM, Balcioglu HE, Schmidt T, Danen EH, Koenderink GH. A guide to mechanobiology: Where biology and physics meet. Biochim Biophys Acta 2015;1853:3043-52.

Jumper N, Paus R, Bayat A. Functional histopathology of keloid disease. Histol Histopathol 2015;30:1033-57.

Kanno T, Takahashi T, Tsujisawa T, Ariyoshi W, Nishihara T. Mechanical stress-mediated Runx2 activation is dependent on Ras/ERK1/2 MAPK signaling in osteoblasts. J Cell Biochem 2007;101:1266-77.

Kawabe J, Okumura S, Nathanson MA, Hasebe N, Ishikawa Y. Caveolin regulates microtubule polymerization in the vascular smooth muscle cells. Biochem

Biophys Res Commun 2006;342:164-9.

Klein EA, Yin L, Kothapalli D, Castagnino P, Byfield FJ, Xu T, et al. Cell-cycle control by physiological matrix elasticity and in vivo tissue stiffening. Curr Biol 2009;19:1511-8.

Kolodney MS, Elson EL. Contraction due to microtubule disruption is associated with increased phosphorylation of myosin regulatory light chain. Proc Natl Acad Sci U S A 1995;92:10252-6.

Lee JA, Choi DI, Choi JY, Kim SO, Cho KA, Lee JB, et al. Methyl-beta-cyclodextrin up-regulates collagen I expression in chronologically-aged skin via its anti-caveolin-1 activity. Oncotarget 2015;6:1942-53.

Lee JY, Yang CC, Chao SC, Wong TW. Histopathological differential diagnosis of keloid and hypertrophic scar. Am J Dermatopathol 2004;26:379-84.

Lee PT, Lin HH, Jiang ST, Lu PJ, Chou KJ, Fang HC, et al. Mouse kidney progenitor cells accelerate renal regeneration and prolong survival after ischemic injury. Stem Cells 2010; 28:573-84.

Lee YS, Hsu T, Chiu WC, Sarkozy H, Kulber DA, Choi A, et al. Keloid-derived, plasma/fibrin-based skin equivalents generate de novo dermal and epidermal pathology of keloid fibrosis in a mouse model. Wound Repair Regen 2016;

24:302-16.

Leight JL, Wozniak MA, Chen S, Lynch ML, Chen CS. Matrix rigidity regulates a switch between TGF-beta1-induced apoptosis and epithelial-mesenchymal transition. Mol Biol Cell 2012;23:781-91.

Lewis CJ, Mardaryev AN, Sharov AA, Fessing MY, Botchkarev VA. The Epigenetic Regulation of Wound Healing. Adv Wound Care (New Rochelle) 2014;3:468-75.

Lin HH, Lin HK, Lin IH, Chiou YW, Chen HW, Liu CY, et al. Mechanical phenotype of cancer cells: cell softening and loss of stiffness sensing. Oncotarget 2015;6:20946-58.

Low JY, Nicholson HD. Epigenetic modifications of caveolae associated proteins in health and disease. BMC Genet 2015;16:71.

Naitoh M, Kubota H, Ikeda M, Tanaka T, Shirane H, Suzuki S, et al. Gene expression in human keloids is altered from dermal to chondrocytic and osteogenic lineage. Genes Cells 2005;10:1081-91.

Nethe M, Hordijk PL. A model for phospho-caveolin-1-driven turnover of focal adhesions. Cell Adh Migr 2011;5:59-64.

Niessen FB, Spauwen PH, Schalkwijk J, Kon M. On the nature of hypertrophic scars and keloids: a review. Plast Reconstr Surg 1999;104:1435-5

Ogawa R, Akaishi S, Huang C, Dohi T, Aoki M, Omori Y, et al. Clinical applications of basic research that shows reducing skin tension could prevent and treat abnormal scarring: the importance of fascial/subcutaneous tensile reduction sutures and flap surgery for keloid and hypertrophic scar reconstruction. J Nippon Med Sch 2011;78:68-76.

Ogawa R, Hsu CK. Mechanobiological dysregulation of the epidermis and dermis in skin disorders and in degeneration. J Cell Mol Med 2013;17:817-22.

Paul RJ, Bowman PS, Kolodney MS. Effects of microtubule disruption on force, velocity, stiffness and [Ca(2+)](i) in porcine coronary arteries. Am J Physiol Heart Circ Physiol 2000;279:H2493-501.

Raaz U, Schellinger IN, Chernogubova E, Warnecke C, Kayama Y, Penov K, et al. Transcription Factor Runx2 Promotes Aortic Fibrosis and Stiffness in Type 2 Diabetes Mellitus. Circ Res 2015;117:513-24.

Radel C, Carlile-Klusacek M, Rizzo V. Participation of caveolae in beta1 integrin-mediated mechanotransduction. Biochem Biophys Res Commun 2007;358:626-31.

Raglow Z, Thomas SM. Tumor matrix protein collagen XIalpha1 in cancer. Cancer Lett 2015;357:448-53.

Rombouts K, Niki T, Greenwel P, Vandermonde A, Wielant A, Hellemans K, et al.

Trichostatin A, a histone deacetylase inhibitor, suppresses collagen synthesis and prevents TGF-beta(1)-induced fibrogenesis in skin fibroblasts. Exp Cell Res 2002;278:184-97.

Rubin J, Schwartz Z, Boyan BD, Fan X, Case N, Sen B, et al. Caveolin-1 knockout mice have increased bone size and stiffness. J Bone Miner Res 2007;22:1408-18.

Russell SB, Russell JD, Trupin KM, Gayden AE, Opalenik SR, Nanney LB, et al. Epigenetically altered wound healing in keloid fibroblasts. J Invest Dermatol 2010;130:2489-96.

Saito T, Nishida K, Furumatsu T, Yoshida A, Ozawa M, Ozaki T. Histone deacetylase inhibitors suppress mechanical stress-induced expression of RUNX-2 and ADAMTS-5 through the inhibition of the MAPK signaling pathway in cultured human chondrocytes. Osteoarthritis Cartilage 2013;21:165-74.

Seifert O, Bayat A, Geffers R, Dienus K, Buer J, Lofgren S, et al. Identification of unique gene expression patterns within different lesional sites of keloids. Wound Repair Regen 2008;16:254-65.

Stroka KM, Konstantopoulos K. Physical biology in cancer. 4. Physical cues guide tumor cell adhesion and migration. Am J Physiol Cell Physiol

2014;306:C98-C109.

Suarez E, Syed F, Alonso-Rasgado T, Mandal P, Bayat A. Up-regulation of tension-related proteins in keloids: knockdown of Hsp27, alpha2beta1-integrin, and PAI-2 shows convincing reduction of extracellular matrix production. Plast Reconstr Surg 2013;131:158e-73e.

Trimmer C, Whitaker-Menezes D, Bonuccelli G, Milliman JN, Daumer KM, Aplin AE, et al. CAV1 inhibits metastatic potential in melanomas through suppression of the integrin/Src/FAK signaling pathway. Cancer Res 2010;70:7489-99.

Tziotzios C, Profyris C, Sterling J. Cutaneous scarring: Pathophysiology, molecular mechanisms, and scar reduction therapeutics Part II. Strategies to reduce scar formation after dermatologic procedures. J Am Acad Dermatol 2012;66:13-24.

Vazquez-Villa F, Garcia-Ocana M, Galvan JA, Garcia-Martinez J, Garcia-Pravia C, Menendez-Rodriguez P, et al. COL11A1/(pro)collagen 11A1 expression is a remarkable biomarker of human invasive carcinoma-associated stromal cells and carcinoma progression. Tumour Biol 2015;36(4):2213-22.

Wang XM, Zhang Y, Kim HP, Zhou Z, Feghali-Bostwick CA, Liu F, et al. Caveolin-1: a critical regulator of lung fibrosis in idiopathic pulmonary

fibrosis. J Exp Med 2006;203:2895-906.

Wang YH, Chiu WT, Wang YK, Wu CC, Chen TL, Teng CF, et al. Deregulation of AP-1 proteins in collagen gel-induced epithelial cell apoptosis mediated by low substratum rigidity. J Biol Chem 2007;282:752-63.

Wei WC, Lin HH, Shen MR, Tang MJ. Mechanosensing machinery for cells under low substratum rigidity. Am J Physiol Cell Physiol 2008;295:C1579-89.

Witt E, Maliri A, McGrouther DA, Bayat A. RAC activity in keloid disease: comparative analysis of fibroblasts from margin of keloid to its surrounding normal skin. Eplasty 2008;8:e19.

Wong VW, Akaishi S, Longaker MT, Gurtner GC. Pushing back: wound mechanotransduction in repair and regeneration. J Invest Dermatol 2011;131:2186-96.

Wong VW, Rustad KC, Akaishi S, Sorkin M, Glotzbach JP, Januszyk M, et al. Focal adhesion kinase links mechanical force to skin fibrosis via inflammatory signaling. Nat Med 2011;18:148-52.

Yang B, Radel C, Hughes D, Kelemen S, Rizzo V. p190 RhoGTPase-activating protein links the beta1 integrin/caveolin-1 mechanosignaling complex to RhoA and actin remodeling. Arterioscler Thromb Vasc Biol 2011;31:376-83.

Yang MT, Reich DH, Chen CS. Measurement and analysis of traction force

dynamics in response to vasoactive agonists. Integr Biol (Camb) 2011;3:663-74

Zhang GY, Yi CG, Li X, Ma B, Li ZJ, Chen XL, et al. Troglitazone suppresses transforming growth factor-beta1-induced collagen type I expression in keloid fibroblasts. Br J Dermatol 2009;160:762-70.

Zhang GY, Yu Q, Cheng T, Liao T, Nie CL, Wang AY, et al. Role of caveolin-1 in the pathogenesis of tissue fibrosis by keloid-derived fibroblasts in vitro. Br J Dermatol 2011;164:623-7.

Ziros PG, Gil AP, Georgakopoulos T, Habeos I, Kletsas D, Basdra EK, et al. The bone-specific transcriptional regulator Cbfa1 is a target of mechanical signals in osteoblastic cells. J Biol Chem 2002;277:23934-41.

Figure legends

Figure 1. Keloid tissues are stiffer than normal tissue, whereas keloid fibroblasts (KFs) are softer than normal fibroblasts (NFs). (a) Western blot results of skin tissue from control subjects (N=6) and keloid patients (N=6). The protein levels of fibronectin (FN), collagen (COL)1A1, COL3A1, COL11A1, and GAPDH (internal control) were analyzed. (b) Quantification results of FN, COL1A1, COL3A1, and COL11A1 from (a). (c) Atomic force microscopy indentation results

of skin tissue dissected from control subjects (N=6) and keloid patients (N=6). (d) Western blot results of NFs and KFs derived from control subjects (N=6) and keloid patients (N=6), respectively. The protein levels of FN, COL1A1, COL3A1, COL11A1 and GAPDH were analyzed. (e) Quantification results of FN, COL1A1, COL3A1, and COL11A1 from (d). (f) Stiffness distribution histograms of NFs (N=8) and KFs (N=8). (g) Atomic force microscopy indentation results of NFs (N=8) and KFs (N=8). *p<0.05, **p<0.01, ***p<0.001.

Figure 2. RUNX2 is highly upregulated in keloid tissues/fibroblasts. (a) Ingenuity pathway analysis results showing the network of RUNX2 and their close interactions with several extracellular matrix proteins and matrix metalloproteinases (MMPs), which were related to wound healing and scar formation. (b) Immunohistochemical staining results for RUNX2 expression in normal skin tissue, normal scar tissue, hypertrophic scar, and keloid tissue (N=4 in each). Bar=100 μm. (c) Percentage of fibroblasts with nuclear RUNX2 in tissues from (b). (d) Representative immunoblots of skin tissue from control subjects and keloid patients. The protein levels of p-RUNX2, RUNX2, and GAPDH were analyzed. (e) Quantification results of p-RUNX2 and RUNX2 from skin tissue of control subjects (N=6) and keloid patients (N=6). (f) Representative immunoblots of NFs and KFs. The protein levels of p-RUNX2, RUNX2, and GAPDH were analyzed. (g)

Quantification results of p-RUNX2 and RUNX2 from NFs (N=6) and KFs (N=6). *p<0.05, **p<0.01, ***p<0.001.

Figure 3. Keloid dermal fibroblasts show hyperresponsiveness to dermal tissue-equivalent matrix stiffness, which causes increased expression of *RUNX2* and *COL11A1*. (a) Immunofluorescence study of NFs and KFs cultured on matrices of varying stiffness for 24 hours. Cells were stained for RUNX2 (green), the nucleus (blue), and F-actin (red). Bar=20 μm. (b) Percentage of cells with nuclear RUNX2 in NFs (N=5) and KFs (N=5) from (a). (c) Western blot results of NFs (N=4) and KFs (N=4) cultured on matrices of varying stiffness for 24 hours. (d) Representative RT-PCR results of NFs (N=3) and KFs (N=3) derived from explants on matrices of varying stiffness at Day 3. The mRNA expressions of *RUNX2*, *COL11A1*, *fibronectin* (*FN*), and *COL3A1* were analyzed. (e) Quantification results of *RUNX2*, *COL11A1*, *FN*, and *COL3A1* mRNA from (d). *GAPDH*-normalized data were compared with those of NFs cultured on 2 kPa PA gel. *p<0.05, ***p<0.001.

Figure 4. Suppression of *CAV1* in NFs causes cell softening, loss of stiffness sensing ability, and increased expression of RUNX2 and FN. (a) Western blot results of NFs transfected with non-targeting control siRNA (siNC) or siCAV1 for 48 h and KFs. (b) Quantification results of CAV1, RUNX2, and FN from (a).

GAPDH-normalized data were compared with those of NFs (N=3) transfected with siNC. *CAV1* knockdown in NFs causes (c) cell softening, (d) inability to change cell stiffness on matrices of varying stiffness. (e) Confocal immunofluorescence images obtained with anti-RUNX2 (green) in NFs and KFs cultured on dishes and treated with si*NC* or si*CAV1* for 24 hours. Bar=50 μm. (f) Percentage of cells with nuclear RUNX2 in dermal fibroblasts from (e). (g) Percentage of cells with nuclear RUNX2 in si*NC*- or si*CAV1*-transfected NFs and KFs grown on PA gels of 20 kPa and 2 kPa for 24 h. (h) Confocal immunofluorescence images obtained with anti-CAV1 (red), anti-RUNX2 (green), and nucleus (blue) in skin tissues from control subjects (N=2) and keloid patients (N=3). Bar=50 μm. (i) Pearson's correlation comparing CAV1 and RUNX2 intensity in skin tissues from (h). *p<0.05, **p<0.01, ***p<0.001.

Figure 5. *CAV1* knockdown promotes migratory ability of NFs. NFs (N=3) and KFs (N=3) were transfected with siNC or siCAV1 for 24 h. After reaching a confluent monolayer, wound healing experiments were performed. (a) Quantification results of wound scratch (0 h) and recovery (8 h and 24 h) from Supplementary Figure S5. Wound recovery (%)=[(wound area at 0 hours–wound area at 24 hours)/wound area at 0 hours]*100%. (b) The representative force maps of fibroblasts under indicated conditions plated on PDMS micropost arrays. The color scale indicates the magnitude of traction force (nN). (c) Quantification results

of total force and force per post generated in cells from (b). (d) Western blot results of NFs or KFs transfected with si*NC* and si*CAV1* for 48 hours. The protein levels of CAV1, pMLC2, MLC2, and GAPDH were analyzed. (e) Quantification results of CAV1, pMLC2, and MLC2 from (d). *p<0.05, **p<0.01.

Figure 6. Epigenetic control of CAV1 impacts on cell mechanics and RUNX2 expression in KFs. (a) Confocal immunofluorescence images of KFs plated onto culture dishes and treated with various doses of TSA for 24 hours. Bar=20 μm. (b) Western blot results of KFs (N=3) under indicated conditions. The protein levels of CAV1, RUNX2, FN, histone H3 acetyl K9 (histone H3AK9), and GAPDH were analyzed. Quantification results of (c) histone H3AK9, (d) CAV1, (e) RUNX2, and (f) FN from (b). GAPDH-normalized data were compared with those of KFs treated with DMSO (TSA 0 μM). Treatment of KFs with 200 nM TSA (g) hindered wound recovery, (h) increased cell stiffness, and (i) decreased the percentage of cells with nuclear RUNX2 on 2 kPa. *p<0.05, **p<0.01, ***p<0.001.

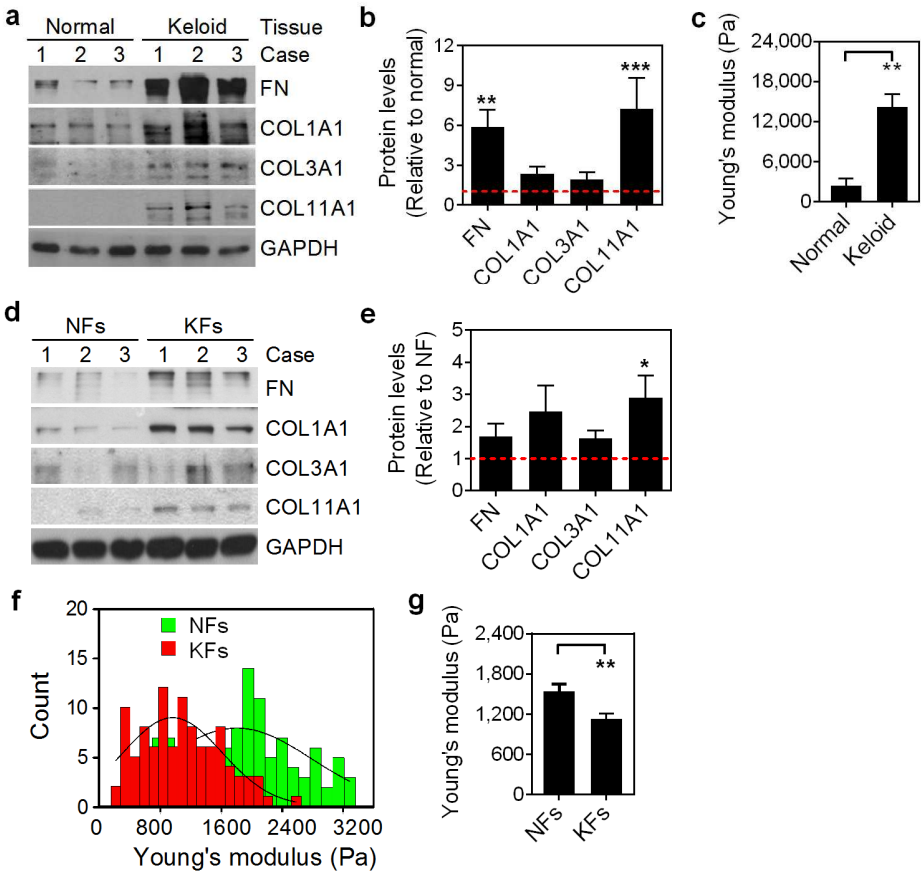

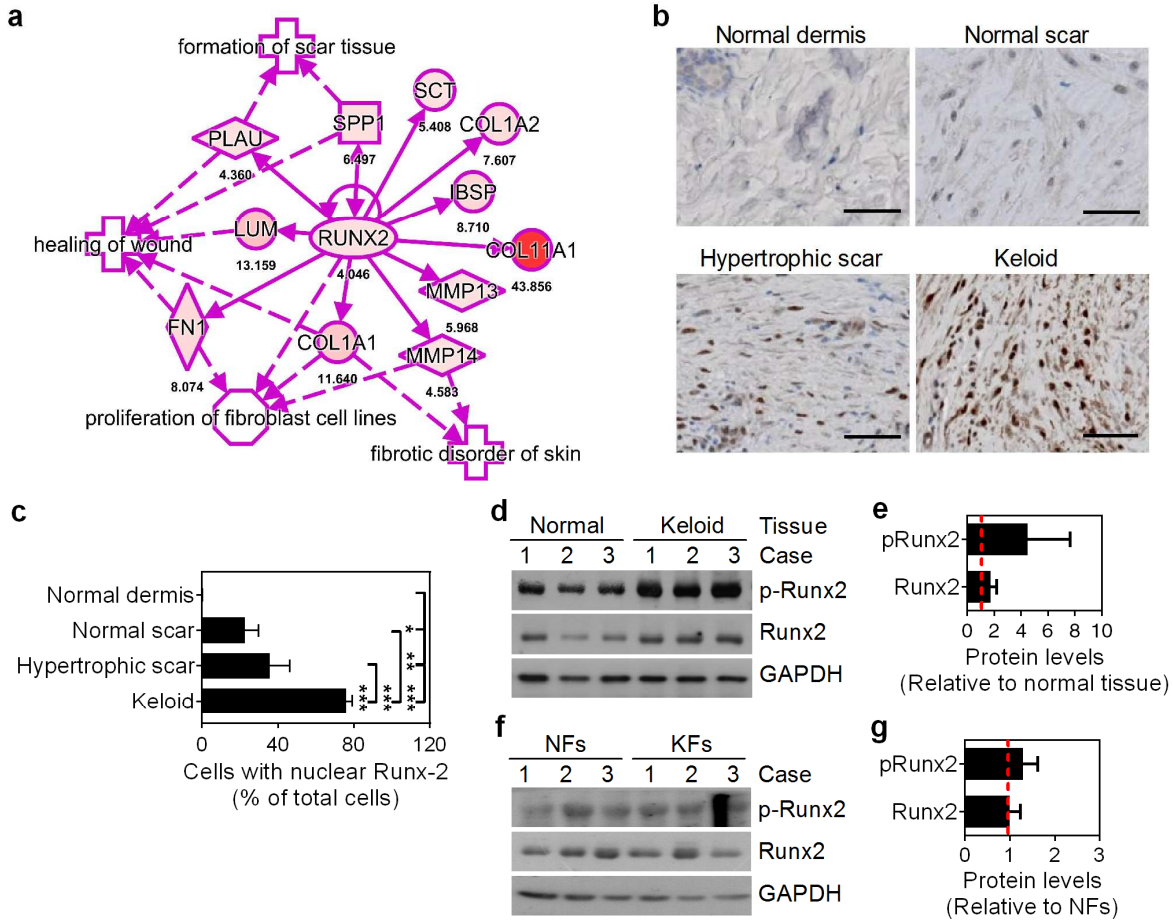
a
formation of scar tissue
SCT
SPP1
5.408
COL1A2
PLAU
6.497
7.607
4.360
IBSP
8.710
healing of wound
LUM
RUNX2
COL11A1
13.159
4.046
43.856
MMP13
5.968
FN1
COL1A1
MMP14
8.074
11.640
4.583
proliferation of fibroblast cell lines
fibrotic disorder of skin
b
Normal dermis
Normal scar
Hypertrophic scar
Keloid
c
Normal dermis
Normal scar
Hypertrophic scar
Keloid
0
40
80
120
Cells with nuclear Runx-2
(% of total cells)
d
Normal
Keloid
Tissue
1 2 3 1 2 3
Case
p-Runx2
Runx2
GAPDH
e
pRunx2
Runx2
0 2 4 6 8 10
Protein levels
(Relative to normal tissue)
f
NFs
KFs
1 2 3 1 2 3
Case
p-Runx2
Runx2
GAPDH
g
pRunx2
Runx2
0 1 2 3
Protein levels
(Relative to NFs)

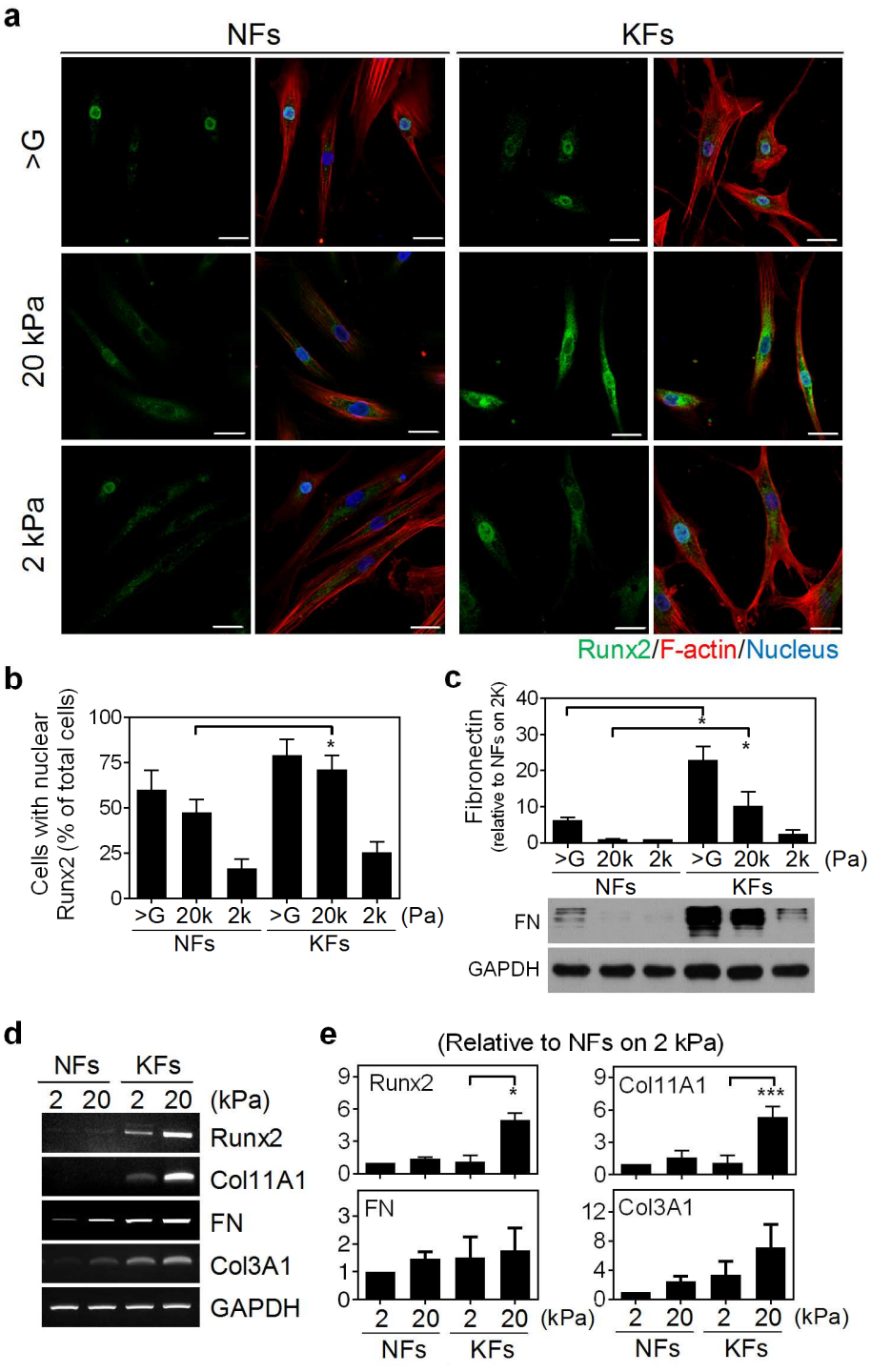
a
NFs
KFs
>G
20 kPa
2 kPa
Runx2/F-actin/Nucleus
b
Cells with nuclear Runx2 (% of total cells)
100
75
50
25
0
>G 20k 2k >G 20k 2k (Pa)
NFs
KFs
c
Fibronectin (relative to NFs on 2K)
40
30
20
10
0
>G 20k 2k >G 20k 2k (Pa)
NFs
KFs
FN
GAPDH
d
NFs KFs
2 20 2 20 (kPa)
Runx2
Col11A1
FN
Col3A1
GAPDH
e
(Relative to NFs on 2 kPa)
Runx2
Col11A1
FN
Col3A1
2 20 2 20 (kPa)
NFs
KFs